

New pH-dependent photosubstitution pathways of syringic acid in aqueous solution: Relevance in environmental photochemistry

Erin Dallin^a, Peter Wan^{a,*}, Erik Krogh^b, Chris Gill^b, Robert M. Moore^c

^a Department of Chemistry, Box 3065, University of Victoria, Victoria, BC V8W 3V6, Canada

^b Applied Environmental Research Laboratories, Department of Chemistry, 900 Fifth Street, Vancouver Island University, Nanaimo, BC V9R 5S5, Canada

^c Department of Oceanography, Dalhousie University, Halifax, NS B3H 4J1, Canada

ARTICLE INFO

Article history:

Received 8 June 2009

Received in revised form 23 July 2009

Accepted 25 July 2009

Available online 4 August 2009

Keywords:

Photosubstitution

Photoprotonation

Humic substance

Membrane introduction mass spectrometry

(MIMS)

Syringic acid

Chloromethane (CH₃Cl)

ABSTRACT

The aqueous photochemistry of 4-hydroxy-3,5-dimethoxybenzoic acid (syringic acid) (**1**) and related compounds has been studied to investigate the novel pH-dependent photosubstitution pathways exhibited upon photolysis. Compounds of this type have previously been shown to produce chloromethane (CH₃Cl) upon photolysis in chloride enriched aqueous solution. Photochemical product studies of **1** and related compounds, along with laser flash photolysis, and membrane introduction mass spectrometry (MIMS) – the latter to directly follow CH₃Cl formation – were employed to study their photochemical behaviour. These studies revealed that the carboxylate form of **1** undergoes a previously unknown photochemical pathway that is initiated by excited state protonation of the benzene ring (*ipso* positions with OCH₃ and OH substituents) by water. The enhanced basicity of the benzene ring at these positions is rationalized by an excited singlet state that has significant charge transfer from the carboxylate anion to the benzene ring, which is corroborated by semi-empirical AM1 (Chem 3D) calculations, as well as by the lack of reaction of the protonated form of **1** and related compounds incapable of this type of charge transfer. The photoproducts observed and/or isolated (CH₃OH derived from the OCH₃ group, 3-methoxygallic acid (**2**), 3,5-dimethoxybenzoic acid (**4**), and CH₃Cl, the latter only when Cl⁻ was added), can be explained by this new photochemical pathway.

© 2009 Elsevier B.V. All rights reserved.

1. Introduction

Dissolved organic matter (DOM) is a class of natural organic compounds containing molecules derived from biota in terrestrial (allochthonous) and/or marine (autochthonous) ecosystems [1]. DOM includes a large assemblage of complex chemical structures characterized by the presence of polyphenols, carboxyls, methoxyls, quinones, carbohydrate and peptide functionalities [2]. Through their ability to absorb sunlight, these substances are known to act as sensitizers or precursors for the production of various reactive species [3], such as hydroxyl radicals [4], singlet oxygen (¹O₂) [5], solvated electrons (e⁻_(aq)) [6], superoxide ion (O₂^{•-}) [7], carbon dioxide [8], hydrogen peroxide [9] and molecular hydrogen [10], in aquatic ecosystems.

In addition, DOM and model lignin compounds have been shown to release a variety of volatile organic compounds (VOCs), including methanol [11] and halomethanes [12]. Methanol is the second most abundant organic gas in the atmosphere after methane with concentrations ranging from 0.1 to 10 ppb_v and an estimated tro-

pospheric lifetime of ~10 days [13], where it is primarily lost by hydroxyl radical oxidation. The predominant sources of atmospheric methanol are biogenic, including plant growth, decay and biomass burning. The contributions from atmospheric oxidation of CH₄ and direct anthropogenic inputs are estimated to be much smaller, while the contribution from hydrolysis of methyl halides is insignificant [14]. Recent measurements of methanol in surface marine waters have put new constraints on methanol sources [15] and have led Millet et al. [16] to suggest that the marine biosphere plays a major role in the global budget. Marine and estuarine environments have been shown to participate in the net transport of halogen to the atmosphere [17] and DOM has been proposed as a carbon source in the photoproduction of halomethanes (e.g., CH₃I and CH₃Cl) [12d,12e]. Chloromethane is the most abundant halogen compound in the atmosphere and is globally mixed at an average concentration of 600 ppb_v [12b]. It has a tropospheric lifetime of 1.4 years [12c] and can consequently migrate into the stratosphere, where it is exposed to high energy photons resulting in the production of chlorine atoms that participate in the regulation of stratospheric ozone [18]. In addition to anthropogenic sources of methyl halides, for example, in manufacturing processes and in the production and use of methyl bromide as a fumigant, a number of natural biotic and abiotic sources have been identi-

* Corresponding author. Tel.: +1 250 721 8976; fax: +1 250 721 7147.
E-mail address: pwan@uvic.ca (P. Wan).

fied. The most important of these include biomass burning [19], wood-rotting fungi [20], coastal salt marshes [21], tropical vegetation [22] and the decomposition of organic matter [12a]. It has been estimated that oceanic sources account for 9–11% [12c].

In addition to the photoproduction of quinones, methanol has been observed in the photochemistry of various lignins and related model compounds [11c]. Recently, Moore has shown that the methoxy group in several lignin model compounds, such as syringic acid (4-hydroxyl-3,5-dimethoxybenzoic acid) can act as a carbon source in the pH-dependent photochemical formation of CH_3Cl in chloride enriched waters [12e]. Structural moieties on syringic acid (**1**) have been identified in terrestrially derived DOM [2a] and as such, **1** serves as an environmentally relevant model for these studies. Opsahl and Benner have shown that aryl-methoxy groups on syringyl moieties of lignin are photochemically labile and preferentially degraded as terrigenous carbon moves from freshwater to the open ocean [23].

Although the photochemical production of halomethanes from DOM has been suggested to involve the photorelease of methyl radicals from aromatic methoxy groups in DOM, and their combination with halogen radicals [12d], direct mechanistic studies on the formation of volatile organohalogenes from model lignin compounds is largely absent. In response to a growing interest in the topic, we have carried out a study of the photochemistry of **1** and related compounds **2–9**, illustrating the details of a proposed mechanism for the formation of VOCs and other photoproducts in de-aerated aqueous solution that is observed from some substrates. We report a mechanistic framework for the photochemical production of methanol and CH_3Cl from syringic acid (and related compounds) in chloride enriched waters initiated by excited state protonation of the benzene ring followed by nucleophilic attack.

2. Experimental details

2.1. General

^1H NMR spectra were recorded on Bruker 300 or 500 MHz instruments in either D_2O or DMSO-d_6 . Mass spectra were recorded using Electrospray Ionization Mass Spectrometry on a Micromass Q-tof *micro* instrument in the negative ion mode with the sample dissolved in neat CH_3OH . pH measurements were taken using a Fisher Scientific Accumet Research Dual Channel pH/Ion meter.

2.2. Materials

All solvents used for synthesis (ACS grade) were purchased from Aldrich and used as received, with distilled water used for photolyses. D_2O and CDCl_3 were purchased from Cambridge Isotope Laboratory. Standard solutions of CH_3Cl (2000 $\mu\text{g}/\text{mL}$) in methanol were supplied in sealed ampules from Fisher Scientific and used as received. All photolyzed compounds and readily available organic and inorganic reagents required in the synthesis reported below were purchased from Aldrich and used as received.

2.2.1. 3-Methoxy-4,5-dihydroxybenzoic acid (**2**)

Methyl gallate (10.1 g, 55 mmol) was dissolved in 800 mL of 5% aq. Borax solution to which a solution of dimethyl sulphate (30 mL) and NaOH (13.2 g in 50 mL water) was added dropwise over 3 h. The black solution was left to stand overnight. The resulting brown solution was then acidified using approximately 25 mL of 40% H_2SO_4 , leaving a clear brown solution with white precipitate. This suspension was extracted continuously with ethyl acetate. Charcoal was used to decolorise the solution before it was concentrated under reduced pressure to leave an orange-brown oil. The resulting material was added to 100 mL of 20% NaOH and refluxed for 1 h. The brown mixture was then acidified with HCl and continuously

extracted with ether to leave a red solution. The crude product was recrystallised three times in hot water (once with charcoal) to give 4.70 g of tan brown crystals. These crude crystals were then recrystallised in hot benzene and methanol to give 1.04 g of **2** as white crystals (10% yield); ^1H NMR (300 MHz, DMSO-d_6) δ 3.78 ppm (s, 3 H, OCH_3), δ 7.02 ppm (d, 1 H, 2-position H), δ 7.07 ppm (d, 1 H, 3-position H), δ 9.04 and 9.28 ppm (s, 1 H each, OH), δ 12.42 ppm (s, 1 H, COOH), ESI-MS m/z 183 (negative ion mode).

2.2.2. Methyl syringate (**3**)

Compound **3** was prepared using a standard Fischer Esterification of syringic acid (**1**) (0.41 g, 2 mmol) with a catalytic amount of H_2SO_4 in 40 mL methanol. The resulting white solution was washed out of the round bottom flask with 35 mL ether and 25 mL H_2O . After draining off the H_2O layer, the ether layer was washed with 4×25 mL 5% NaHCO_3 and 25 mL H_2O . The ether layer was dried with MgSO_4 , with the solvent evaporated under reduced pressure. The reaction yielded 0.40 g of **3** as white crystals (91% yield); ^1H NMR (300 MHz, CDCl_3) δ 3.87 ppm (s, 3 H, ester CH_3), δ 3.91 ppm (s, 6 H, OCH_3), δ 7.29 ppm (s, 2H, Ar H).

2.3. General photolysis procedure

All NMR scale and preparative scale photolyses were carried out in a Rayonet RPR 100 photochemical reactor equipped with 16×300 nm lamps. The solutions were purged with argon for inert atmosphere experiments or air using a stainless steel needle for approximately 10 min prior to photolysis. Preparative scale photolyses were also continuously purged during irradiation. All photolysis experiments ranged from 30 min to 10 h depending on the experiment. No dark reactions were observed for all compounds studied.

2.3.1. NMR scale photolysis of syringic acid (**1**) and related compounds

For NMR scale photolysis, the solutions were contained in a closed quartz tube (~ 25 mL) which was cooled to approximately 15°C using an external water bath. After photolysis, the reaction mixture was transferred without workup to an NMR tube using a Pasteur pipette (for CH_3OH measurement) or a gas tight syringe (for CH_3Cl measurement).

For the photolysis of compounds **1–9** in which the yield of CH_3OH was measured, 10 mg of compound was dissolved (using a sonicator) in approximately 9 mL D_2O and 1 mL CD_3CN to a concentration of 10^{-3} to 10^{-4} M (some compounds required varying ratios of solvent). The pH was then adjusted as necessary using 0.1 M NaOD or 0.1 M D_2SO_4 . If the photolysis required an added ion (Cl^- , I^- or CN^-), this was added as NaCl, NaI or KCN, respectively, to achieve 0.5 M in the reaction mixture. ^1H NMR of the reaction mixture showed the formation of CH_3OH for $\text{pH} > 4$ as measured by the signal at δ 3.3–3.4 ppm (this shift varied slightly if the ratio of D_2O to CD_3CN differed), confirmed by adding neat CH_3OH (and observing the relative increase in the CH_3OH integration by ^1H NMR) and MIMS experiments. Methanol conversions were measured by integration of the methyl signals produced by ^1H NMR at δ 3.3–3.4 ppm).

2.3.2. Preparative scale photolysis of syringic acid (**1**)

Preparative scale photolyses were conducted at 300 nm (typically, 1–3 h) in a ~ 150 mL open quartz tube that was maintained at 15°C with an internal cold finger. The general workup of the reaction mixture involved acidification using 1 M HCl if the pH was greater than 7 followed by extraction using 4×50 mL CH_2Cl_2 , drying of the organic layer over MgSO_4 , filtering to remove the drying agent and evaporation of the solvent under reduced pressure.

For the photolysis of **1** in which the photoproducts were isolated, 20 mg of **1** was dissolved in 100 mL of H₂O, with the mixture adjusted to the appropriate pH using 1 M NaOH or 1 M H₂SO₄. After workup, the dried photomixture was dissolved in DMSO-d₆ for ¹H NMR analysis, or dissolved in CH₃OH for analysis by ESI-MS.

2.3.3. Preparative scale photolysis of 3,4,5-trimethoxybenzoic acid (**5**)

The preparative scale photolysis of **5** involved preparing a solution made by dissolving 29 mg of **5** in 100 mL H₂O and adjusting to pH 8 using 1 M NaOH. After photolysis, the entire photomixture was made acidic with H₂SO₄, extracted with 4 × 50 mL CH₂Cl₂, dried over MgSO₄, filtered and evaporated under vacuum. The dried photolysate was then dissolved in DMSO-d₆ for ¹H NMR analysis.

2.4. Product quantum yields

Product quantum yields for the formation of CH₃OH from the photolysis of **1** and **5** were determined using the photodemethoxylation of 1,2-dimethoxybenzene as a secondary actinometric standard. The yield of CH₃OH from the photolysis of 1,2-dimethoxybenzene ($\Phi_p = 0.016$ at pD 1.3, 254 nm [24]) were compared to those for **1** and **5** to assess the quantum yield of methanol production. Solutions of **1**, **5** and 1,2-dimethoxybenzene were made by dissolving a known amount of compound into 1:1 D₂O-CD₃CN so that the concentrations were 5.1×10^{-3} M. The solution of 1,2-dimethoxybenzene was adjusted to pD 1.3 using D₂SO₄ and the pD of **1** and **5** adjusted to 8 with NaOD. The solutions were Ar purged prior to photolysis for 10 min and then photolyzed at 254 nm (14 lamps) for 1 h in a closed quartz tube that was cooled with an external water bath to <15 °C. After photolysis, 750 μL of the solution was removed by syringe from the reaction mixture to an NMR tube with 1.0 μL of acetone added as an internal standard. A ¹H NMR of this mixture was immediately taken to measure the amount of CH₃OH relative to the internal standard. All three compounds were photolyzed on the same day using the same lamps, Rayonet and quartz tube.

2.5. Membrane introduction mass spectrometry (MIMS)

MIMS data were obtained using a quadrupole ion-trap mass spectrometer (Polaris-Q™, Thermo-Electron, San-Jose, CA, USA) equipped with a capillary hollow fibre polydimethylsiloxane (PDMS) interface constructed in-house with sample flowing over the outside of the membrane (10.0 cm length; ID 0.51 mm; OD 0.94 mm, Silastic brand®, Dow Corning, Midland, MI) [25]. Reactions were monitored by re-circulating the headspace above the photolysis solution in a closed loop through 0.25 in. O.D. Teflon tubing using a peristaltic pump (model 77200-62 Easy-Load II Masterflex; Cole-Palmer, Concord, ON, Canada with LS 25 Viton™ pump tubing) returning the headspace gases below the level of the photolysis solution at a sampling flow rate of 375 mL/min. Since the proportion of CH₃Cl in the headspace and solution is constant at the constant volume fractions and temperature employed in these experiments, the amount of CH₃Cl measured in the headspace is representative of the concentration in solution. A helium sweep gas flowing through the lumen of the capillary hollow fibre membrane transports the permeate molecules to the mass spectrometer for real-time monitoring. Ionization was achieved with an external EI ion source at 70 eV. This instrument was employed to continuously monitor the volatile and semi-volatile photoproducts using full scan and selected ion monitoring (SIM) modes. CH₃Cl, carbon dioxide and methanol were monitored using SIM at $m/z = 50 + 52$, 44 and 32, respectively. The MS lenses were tuned on a mass of 51, for the collection of CH₃³⁵Cl⁺ ($m/z = 50$) and CH₃³⁷Cl⁺ ($m/z = 52$) based on comparison to the NIST mass spectrum.

Calibrations were performed by injecting CH₃Cl standards (2000 μg/mL in methanol, Fisher Scientific) into the aqueous phase of a closed reaction vessel and allowing the equilibration of the CH₃Cl with the headspace (at a constant temperature), using the same volume fractions of headspace to reaction vessel. The t_{10-90} risetime for the CH₃Cl to reach a steady state signal under these conditions is 60 s, which provides a lower limit on the temporal resolution of our MIMS experiments. Plotting the nominal aqueous phase concentration against the steady state MIMS signal (SIM; $m/z = 50, 52$) from the re-circulated headspace yielded a straight line ($y = 2.86 \times 10^9 \text{ M}^{-1} x - 22.0$, $R^2 = 0.999$) over a range of 0.1–1.4 μM CH₃Cl. Detection limits for CH₃Cl under these experimental conditions were estimated to be 20 nM based on S/N = 3. Control experiments showed no hydrolytic or photochemical (300 nm) loss of authentic aqueous CH₃Cl over the pH range and temperature conditions employed in these experiments.

MIMS photolysis experiments were conducted in a closed ~800 mL quartz vessel equipped with an internal cold finger and two side arm inlets positioned inside of a Rayonet RPR-100 photochemical reactor (Southern New England Ultraviolet Company, Brandford, CT) equipped with eight 300 nm lamps. Solutions of **1** were made by dissolving 40 mg in 400 mL (500 μM) of deionized water (sonication used to aid in dissolution) with 0.5 M Cl⁻ and adjusted to the desired pH by using either NaOH or HCl. Prior to mixing the solutions, the water was purged with the desired gas (N₂ or air) for 1.5 h. For experiments in the absence of O₂, the headspace of the photolysis tube (~400 mL headspace for 400 mL solution) and tubing leading to the MIMS was flushed with N₂ to ensure that no residual air remained. A cold finger inserted into the photolysis tube kept the temperature of the solution at 20 °C using

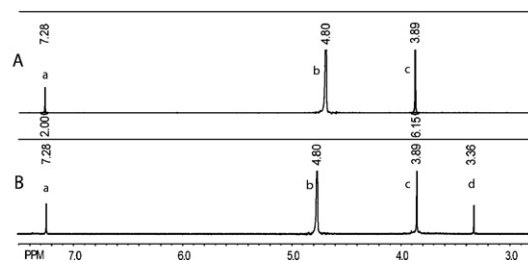
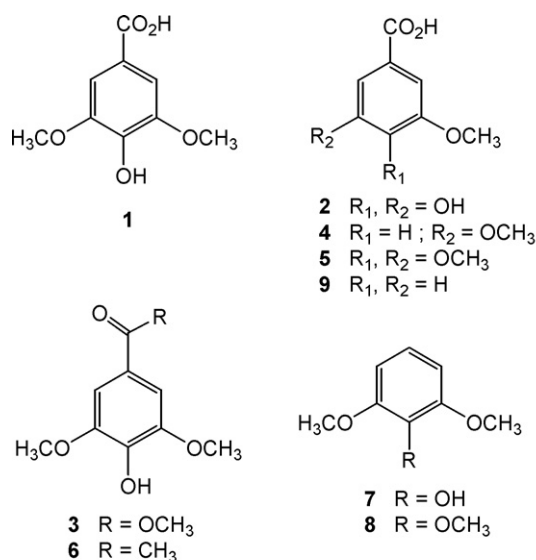


Fig. 1. 300 MHz ¹H NMR spectra in D₂O for the 300 nm aqueous photolysis of **1** at pD 7. (A) Un-irradiated **1**; (B) **1** irradiated for 3 h. Signal a (aromatic protons) corresponds to **1**, b is NMR solvent, c (methoxy protons) is from **1** and d corresponds to CH₃OH.

a thermostat controlled water bath (Forma Scientific 2095 Bath and Circulator), re-circulated using a peristaltic pump (described above). Before beginning any experiment, the baseline signal was stabilized for a minimum of 10 min.

2.6. Laser flash photolysis (LFP)

All transient spectra were recorded using nanosecond LFP with excitation using a Spectra Physics Nd:YAG laser (Model GCR-12, frequency quadrupled to yield 266 nm excitation), with static cell (1 cm², quartz) measurements. Prior to photolysis, the solution was purged with either N₂, O₂ or N₂O for 30 min.

3. Results and discussion

3.1. Product studies

Previous studies have reported the formation of CH₃Cl upon irradiation of **1** in chloride enriched water by purge and trap GC/MS techniques [12e]. NMR scale photolysis of **1** in D₂O containing 0.5 M Cl⁻ failed to detect the presence of CH₃Cl under both aerated and de-aerated conditions (see description in Section 2.3.1). However, these experiments did reveal the formation of CH₃OH, as evidenced by the growth of the characteristic singlet at δ 3.36 ppm (¹H NMR) due to the methyl group of CH₃OH (Fig. 1) (~10% yield after 2 h photolysis; 20% yield after 10 h). This was confirmed by injection of an authentic sample of CH₃OH which resulted in superimposed methyl peaks in the ¹H NMR spectrum. Photolysis of **1** with aqueous I⁻ and CN⁻ also led to the formation of CH₃OH as opposed to CH₃I or CH₃CN, respectively. Likewise, photolysis of **1** in neutral aqueous solution without added Cl⁻, I⁻ or CN⁻ also gave CH₃OH. Repeated attempts to identify CH₃Cl in sealed NMR scale experiments led us to the conclusion that the quantum yield for production was sufficiently low that its production was below the NMR detection limits under the conditions employed.

The identities of the aromatic (i.e., benzene ring-derived) products from the photolysis of **1** in neutral aqueous solution were determined using a preparative scale photolysis (see description in Section 2.3.2), where the products were identified using Electrospray Ionization Mass Spectrometry (ESI-MS) and ¹H NMR. The ESI-MS analysis of this reaction mixture in negative ion mode (in CH₃OH) revealed the mass for **1** at 196.9 g/mol with smaller intensity mass signals at 182.9 g/mol corresponding to the demethylated derivative **2**, 181.1 g/mol for the dehydroxylated derivative **4** and 349.3 g/mol that could be associated with a decarboxylated biphenyl derivative **10** (vide infra). The product yields as determined by NMR were 8%, 4% and 5% for compounds **2**, **4** and **10**, respectively.

To determine if the formation of CH₃OH from the methoxy groups of **1** was technically a demethoxylation or a demethylation (i.e., cleavage occurring at the C_{aryl}-O or the C_{methyl}-O bond, respectively), photolysis of **1** was conducted in 26 atom % ¹⁸O labelled water (pH 8). This led to an increase in the intensity of the M+2 peak observed for **2** (from 0 to 10%, relative to the base peak at M⁺) compared to a control experiment (measured by ESI-MS in CH₃OH, negative ion mode), indicating that the mechanism clearly involved a demethoxylation, since the ¹⁸O was incorporated into the photoproduct **2** (formation of **2**-³¹⁸O) (Eq. (1)) (a demethylation would not have resulted in ¹⁸O incorporation), although a competing demethylation pathway cannot be ruled out since we were not able to confirm isolation of up to the required 26% ¹⁸O label in product **2** the is required for a wholly demethoxylation pathway. Additionally, we could not confirm the operation of a demethylation pathway (with water as nucleophile; vide infra when Cl⁻ is used as nucleophile) since our method was incapable of detecting for formation of CH₃¹⁸OH that would be formed in this case.

Table 1

Yield of CH₃OH for the aqueous photolysis of the various compounds at 300 nm in pD 7, quantified by 300 MHz ¹H NMR integration of the CH₃OH signal relative to acetone as an internal standard.

Compound	% Yield CH ₃ OH	Φ_p
1	14	0.010 ^a
2	14	–
5	4.0	0.006 ^a
6	1.8	–
1 (pD 4)	0.7	–
3	0.5	–
4, 7, 8, 9	0.0	–

^a Measured relative to the Φ_p for demethylation of 1,3-dimethoxybenzene as a secondary standard, by measuring for the amount of CH₃OH produced (λ_{ex} 254 nm) [24].

When **1** was photolyzed in H₂O the aromatic signals in the ¹H NMR of **4** shows a new characteristic doublet (δ 7.05 ppm, 2H) and a triplet (δ 6.74 ppm, ¹H) associated with its two ortho and one para protons, respectively. A preparative scale photolysis of **1** in D₂O revealed that the proton that replaced the hydroxy group (at the para position) in **1** came from the water (Eq. (2)), since the ¹H NMR of the photoproduct **4**-*d* revealed a loss of the *meta* coupling to a proton (singlet at δ 7.05 ppm, 2H), and absence of the triplet signal at δ 6.74. The formation of the dehydroxylated product **4** also occurs when the structurally related 3,4,5-trimethoxybenzoic acid (**5**) was photolyzed in aqueous solution. Preparative scale photolysis of **5** revealed that **1** and **4** were formed in a 2% and 44% yield, respectively (Eq. (3)); CH₃OH was also formed from **5**, vide infra). We have ruled out the possibility that **4** is formed via secondary photolysis of **1** since the product ratio above was observed even at low conversions.

The carboxylic acid moiety in **1** (and **5**) can exist as the acid or as the carboxylate ion, depending on the pH, which may have an effect on the outcome of the photochemistry. Therefore, we examined the effect of pH on the observed photochemistry. The trend observed in Fig. 2 was revealed by photolyzing **1** over pH 2–10 and monitoring the ¹H NMR integration of the CH₃OH signal at δ 3.36 ppm relative to an acetone internal standard. In acidic conditions (below pH 4) there was no detectable yield of CH₃OH, while in pH > 8, the yield of demethoxylation reached a maximum. This trend, where the demethoxylation occurs at pH > 4 correlates well to the pK_{a1} of **1** at 4.34 [26] and indicates that the demethoxylation reaction occurs only when **1** is in the carboxylate form. The other products observed during the photolysis of **1** (i.e., **2**, **4** and **10**) were identical under basic and neutral conditions suggesting that the same mechanism is operative regardless of the pH once the pH is > 4. Quantum yields for the production of methanol (Φ_{CH_3OH}) were determined for **1** and **5** to be 0.010 and 0.0058, respectively (Table 1) by comparison to the conversion of 1,2-dimethoxybenzene to 2-methoxyphenol.

To further investigate the mechanism for the demethoxylation, structurally similar compounds were studied to explore what functionalities were essential in the photochemical formation of CH₃OH. Four other compounds in the series were found to give methanol on photolysis: **2**, **3**, **5** and **6**, at yields of 14%, 0.5%, 4% and, 1.8%, respectively (Table 1). Of note is that compounds **4**, **7**, **8** and **9** failed to give detectable amounts of CH₃OH (in neutral pH).

The photochemical production of CH₃OH from the methyl ester **3** and ketone **6** drops by more than an order of magnitude when compared to **1** under identical conditions (pD 7, 1 h photolysis, 300 nm) suggesting that the electronic effect of the functional group at the 1-position plays an important role in the demethoxylation reaction (Table 1). Furthermore, when the protonated form of **1** (at pD 4) is photolyzed the yield of methanol is only 0.7%, similar to that observed for the methyl ester **3**. Indeed, photolysis of compounds **7** and **8**, which no longer have the carboxyl group, showed no observable CH₃OH production.

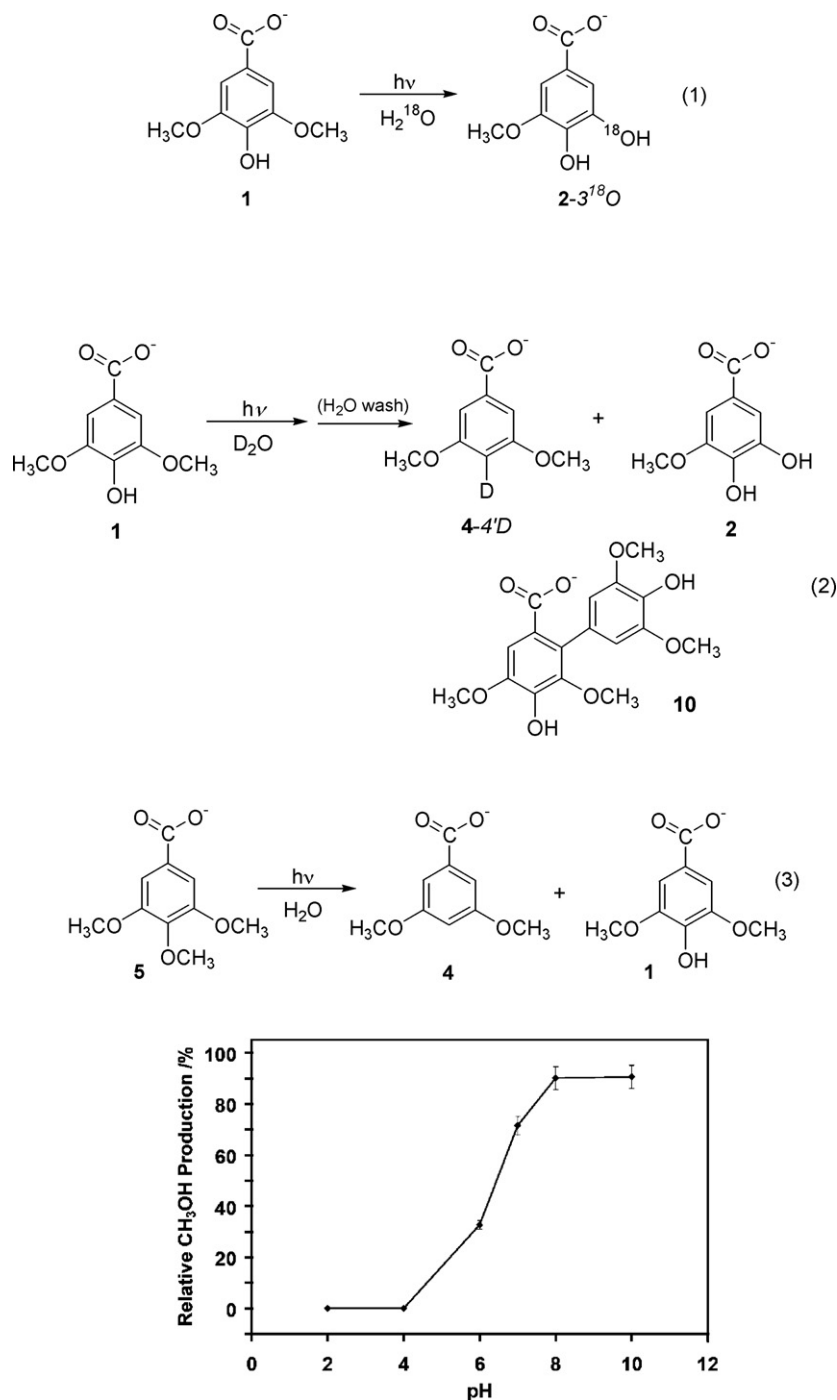


Fig. 2. Yield of CH_3OH on the photolysis of **1** in D_2O vs. pH (pD) (as measured by the integration of the 300 MHz ^1H NMR signal for CH_3OH at δ 3.36 ppm, relative to an acetone internal standard).

The photochemical production of CH_3OH also appears to require three electron donating groups present in **1** (i.e., methoxy or hydroxy), since the photolysis of **2** and **5** both produce CH_3OH (Table 1). If one or two of these donating groups is replaced with a hydrogen (as in **4** or **9**), the reaction was not observed. We postulate that three electron donating (OR, R = H or CH_3) substituents are required in order to sufficiently stabilize a critical intermediate in the demethoxylation pathway (vide infra).

3.2. Membrane introduction mass spectrometry (MIMS)

In this work, we report the first use MIMS as an *on-line* reaction monitoring strategy, to directly observe the formation of CH_3Cl

during the photolysis of syringic acid (**1**). Although ^1H NMR (vide supra) failed to detect the photochemical formation of CH_3Cl in Cl^- enriched water, use of MIMS was ultimately successful in its detection, albeit in low quantities. Thus, photolysis of aqueous solutions containing **1** supplemented with Cl^- re-circulated in a closed loop over a semi-permeable membrane interfaced to an ion-trap mass spectrometer showed the steady evolution in the SIM signal at $m/z = 50, 52$ consistent with the mass spectrum of authentic CH_3Cl . A series of control experiments where either **1**, Cl^- or the UV were absent showed no observable increase at $m/z = 50, 52$ indicating that all three are essential for CH_3Cl formation.

The photolysis of **1** in chloride supplemented solution at pH 7 lead to a roughly linear increase in the concentration of CH_3Cl up

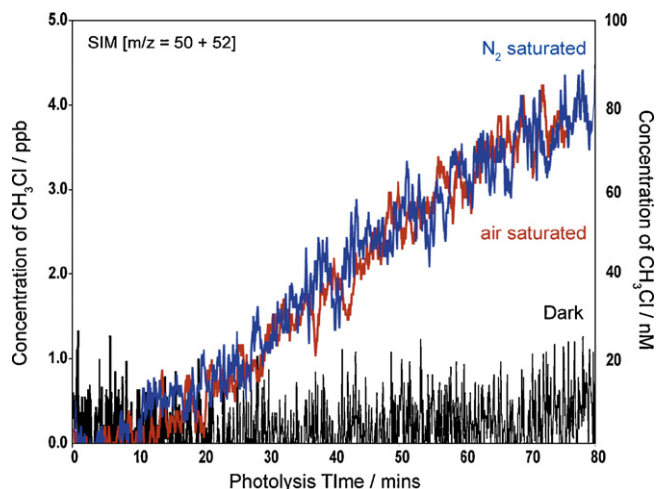


Fig. 3. CH₃Cl production as monitored by closed loop MIMS, during 300 nm photolysis of 500 μM **1** in aqueous solution at pH 6 supplemented with 0.5 M Cl⁻ purged with air, N₂ and dark control experiment (SIM; *m/z* = 50, 52).

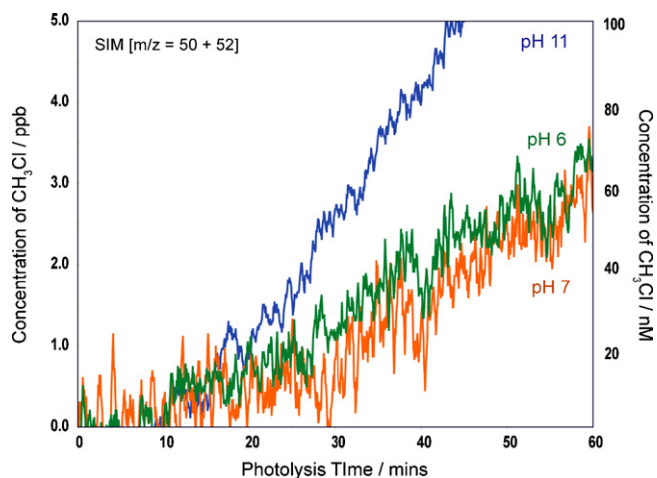


Fig. 4. CH₃Cl production as monitored by closed loop MIMS, during 300 nm photolysis of 500 μM of **1** in aqueous solution at pH 6, 7 and 11 supplemented with 0.5 M Cl⁻ (SIM; *m/z* = 50, 52).

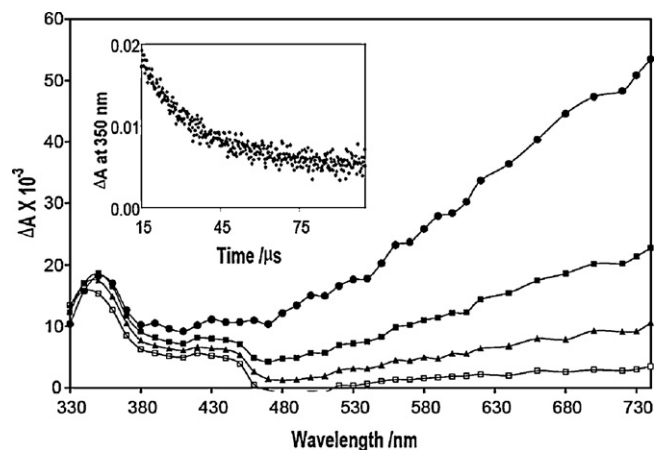


Fig. 5. Transient absorption spectra of **1** in pH 10 purged with N₂; time after laser pulse: (●) = 0.63 μs, (■) = 3.2 μs, (▲) = 6.3 μs, (□) = 13 μs. (Inset: transient decay taken at 2.0 × 10⁻⁴ ns intervals at λ = 350 nm, τ = 5 μs.)

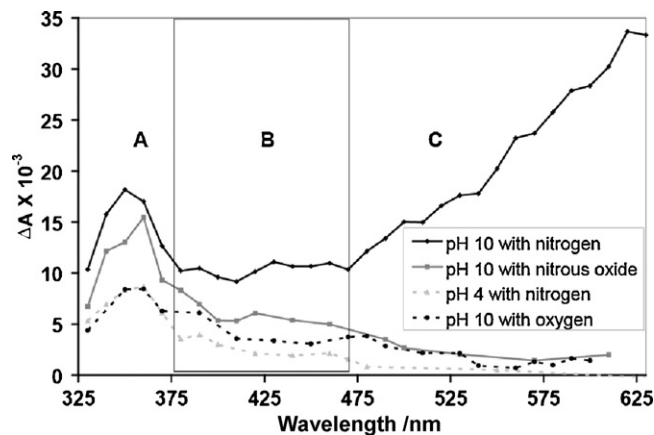


Fig. 6. Comparison of the transient absorption spectra for **1** in H₂O at pH 4 and 10 (approximately 1 μs after the laser pulse). Transient lifetimes in windows (A–C): (A) pH 10 (N₂), pH 10 (N₂O), pH 10 (O₂) and pH 4 (N₂) at 38 μs, 5 μs, 0.2 μs and 4 μs, respectively; (B) pH 10 (N₂) and pH 10 (N₂O) at 8.5 μs and 6.2 μs, respectively (no transient for pH 10 (O₂) or pH 4 (N₂)); (C) solvated electron present in only the pH 10 (N₂) sample with a lifetime of 3.5 μs.

to 80 μM over an 80 min photolysis in both aerated and de-aerated solutions (Fig. 3). We observed little difference in CH₃Cl formation when the solution is de-aerated with N₂. Since O₂ is a known triplet and methyl radical quencher and electron scavenger, this result suggests that triplets, methyl radicals and free electrons are not intermediates in the pathway to form CH₃Cl. Calibration of the SIM signal and integrating over 60 min leads to a rate of CH₃Cl production of 60 (±10) nM h⁻¹. Given that the solution concentration of **1** was 500 μM, this corresponds to a rate of CH₃Cl production of 120 (±20) μM M⁻¹ h⁻¹. It should be noted in addition to the CH₃Cl and CH₃OH production, we also observe an increase in MIMS selected ion monitoring signal at *m/z* = 44 (data not shown), which we attribute to the photochemical production of CO₂ as a result of a concurrent photodecarboxylation of **1** which we believe leads to **10**.

The photochemical production of CH₃Cl from **1** was monitored at several pHs in de-aerated solution (Fig. 4) and found to be pH sensitive. At pH 6 and 7 the rate of CH₃Cl production is estimated

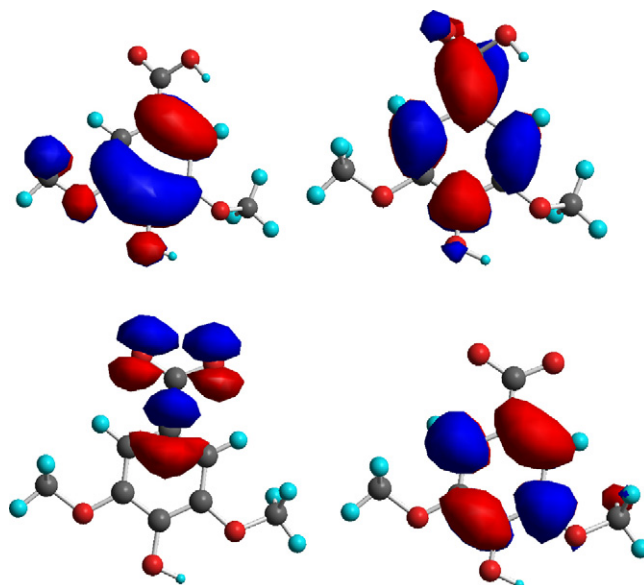


Fig. 7. Calculated HOMO (left) and LUMO (right) (AM1, Chem 3D) for syringic acid (**1**), (top) acid form (ArCO₂H); (bottom) carboxylate form (ArCO₂⁻).

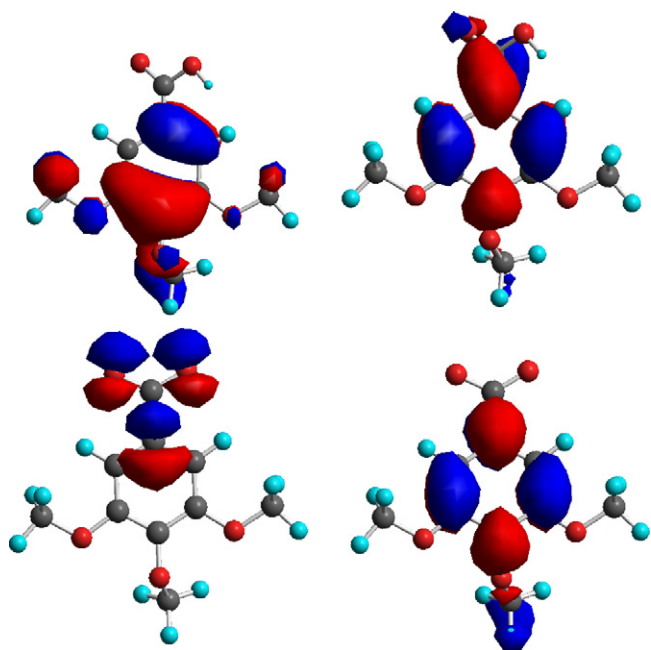


Fig. 8. Calculated HOMO (left) and LUMO (right) (AM1, Chem 3D) for 3,4,5-trimethoxybenzoic acid (**5**), (top) acid form (ArCO_2H); (bottom): carboxylate form (ArCO_2^-).

to be $60 (\pm 10 \text{ nM h}^{-1})$, whereas at pH 11 production rates increase to $160 (\pm 30 \text{ nM h}^{-1})$. This is consistent with preliminary work by Moore [12e], which showed an approximate three fold increase in CH_3Cl production between a pH of 5.0 and 7.7 in aerated solution using off-line quantification via purge and trap GC/MS.

Using the CH_3Cl production from the MIMS experiment, we estimate the upper limit for % conversion to CH_3Cl to be no greater than 0.01%, which is much smaller than that of CH_3OH (13.8% at $\text{pH} > 7$) under similar conditions. Because the production of CH_3Cl was so small, it was not possible to measure an accurate quantum yield. However, based on the quantum yield determined for the production of methanol and the relative conversions to CH_3Cl and CH_3OH , we estimate an upper limit for the quantum yield for CH_3Cl from **1** in de-aerated 0.5 M aqueous chloride ion to be on the order of 10^{-5} .

3.3. Laser flash photolysis (LFP)

LFP studies were carried out for **1** and **5** under a variety of conditions. LFP of **1** in H_2O at pH 10 (N_2 purged) showed three transient absorptions (Fig. 5). Although we have not definitively identified the transients at 350 nm ($\tau = 5 \mu\text{s}$) and 430 nm ($\tau = 8.5 \mu\text{s}$) (vide infra), we have assigned the broad transient at $\lambda > 500 \text{ nm}$ to the solvated electron based on the following observations. When **1** was photolyzed in H_2O at pH 10 in the presence of efficient electron

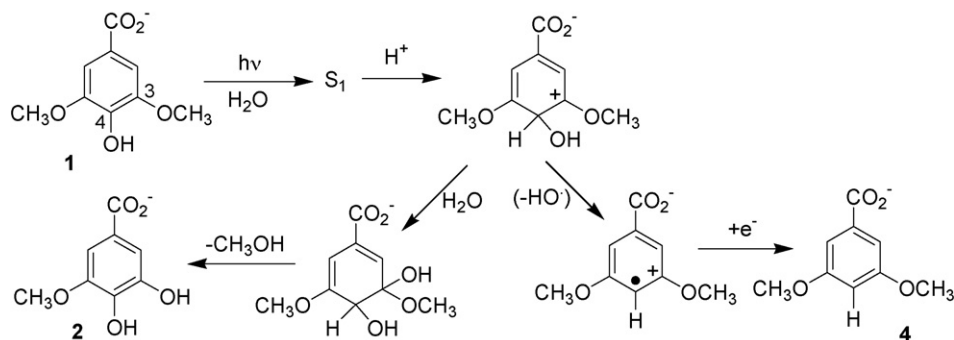
acceptors such as N_2O or O_2 this transient does not appear, thereby supporting its identification as the solvated electron ($e^-_{(\text{aq})}$). Fig. 6 shows the comparison of the LFP for **1** in basic aqueous solution (pH 10) purged with N_2 , N_2O and O_2 as well as at pH 4 in an N_2 purged solution. The solvated electron appears only when **1** is photolyzed in N_2 purged solution at pH 10. The transient at 350 nm, which has a lifetime of $38 \mu\text{s}$ in the presence of N_2 is rapidly quenched ($\tau \sim 0.2 \mu\text{s}$) in the presence of O_2 (an effective triplet quencher). The absence of the solvated electron and the quenching of the transient at 350 nm in the presence of O_2 , suggest that the transient at 350 nm is probably the triplet state.

We have also carried out LFP experiments on **5** since it undergoes similar photochemistry to **1** (i.e., both demethoxylation and hydroxylation). Compound **5** exhibited a transient absorption at 320 nm with a lifetime of $4 \mu\text{s}$ which is similar to the transient observed in the LFP of **1** under similar conditions ($\lambda_{\text{max}} \sim 350 \text{ nm}$, $\tau \sim 5 \mu\text{s}$). Furthermore, this transient was effectively quenched by O_2 , similar to the behaviour of the 350 nm transient observed during the LFP of **1**. In LFP experiments of lignin and other model compounds, researchers have assigned transients with maxima at 410 and 460 nm to phenoxy and ketyl radicals, formed from a bimolecular hydrogen abstraction via triplet state aromatic carbonyls [27]. They also observe transients with maxima $< 400 \text{ nm}$ similar to those that we observe in the photolysis of **1** and **5**, which we suspect are triplet states that are not involved in the demethoxylation or dehydroxylation products **2** and **4**, respectively.

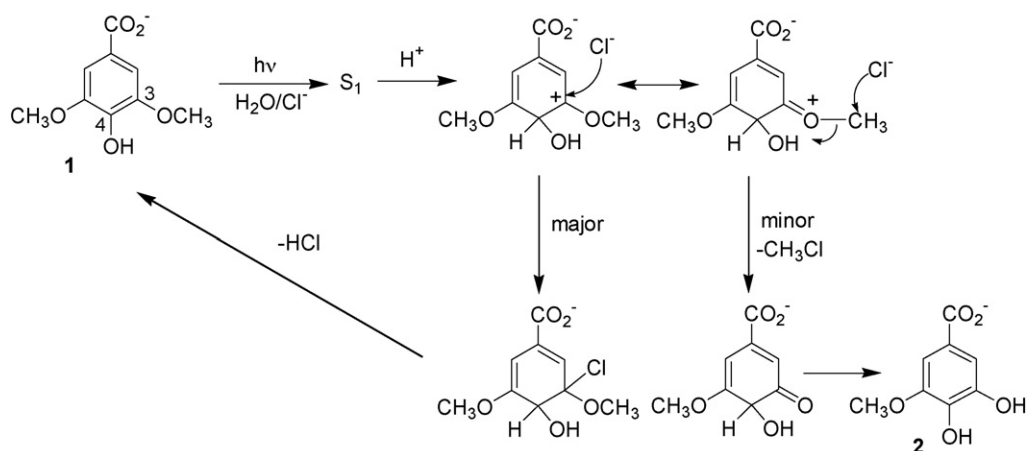
In contrast to **1**, the LFP of **5** did not result in the appearance of detectable amounts of the solvated electron in basic solution. Since **5** has been shown to undergo photodemethoxylation, but does not photorelease an electron in the LFP experiments, it would appear that the solvated electron is not important in the photochemical production of methanol. We suggest instead that the $e^-_{(\text{aq})}$ is associated with the formation of the biphenyl product **10**. Photoejection of an electron from either the carboxylate or phenoxide ion of **1**, followed by decarboxylation and coupling with another molecule of starting material will yield **10**. Since we do not observe the solvated electron or biphenyl product in the photolysis of **1** under acidic conditions or from **5**, we propose that the photoejection of an electron occurs from the dianionic form of **1**. We estimate the $\text{pK}_{\text{a}1}$ and $\text{pK}_{\text{a}2}$ values for **1** to be $4.3 (\pm 0.1)$ and $9.3 (\pm 0.2)$ [26], respectively, suggesting that the dianionic form will predominate at pH 10. The initially formed phenoxyl radical leads to the observed formation of CO_2 and biphenyl **10**. Since **5** is lacking the hydroxyl group in the 4-position, it would not be able to participate in this mechanism, thus accounting for the absence of the solvated electron and biphenyl products.

3.4. Mechanisms of reaction

Based on the results from product studies, and in conjunction with LFP and MIMS data, we propose a mechanism for the pho-



Scheme 1.



Scheme 2.

tochemical production of compounds **2** and **4** from syringic acid along with the release of CH_3OH and CH_3Cl in aqueous solution that is based on a primary photochemical step involving protonation (by water) of the benzene carbons *ipso* to the methoxy (or hydroxyl) of **1** and **5**. The basis for this primary step is not intuitively obvious but is well supported by examination of calculated HOMOs and LUMOs (AM1, Chem 3D/MOPAC) for **1** and **5** (acid and carboxylate ion forms) (Figs. 7 and 8). As shown in Figs. 7 and 8, electronic excitation of the carboxylate forms of these compounds would result in substantial charge migration from the carboxylate ion to all the benzene ring carbon atoms. In particular, a cursory examination would predict that carbons 3, 4 and 5 would experience the greatest increase in basicity (electron density) for both compounds. Note that for the acid forms, there is charge migration away from the benzene ring, into the carboxylic acid group. This latter finding also correlates well with the lack of reaction from the acid forms of these compounds. Although more sophisticated theoretical methods are possible, these simple calculations are sufficient to demonstrate the anticipated reactivity of these compounds.

Shown in Scheme 1 is the proposed mechanism for reaction of the parent compound **1** that would give rise to photoproducts **2** and **4**. The first step involves protonation of the benzene ring at either carbons 3 or 4 in the excited singlet state (*vide infra*). Protonation at carbon 3 would lead to an arenium ion (not shown) with the positive charge localized next to the carbon adjacent to the 4-OH substituent. This intermediate would not lead to any new product since it would suffer nucleophilic attack by water at this carbon. Subsequent loss of water would lead to starting material. Protonation at carbon 4 would lead to the arenium ion shown in Scheme 1. Nucleophilic attack by water at the positive charge localized at carbon 3 would lead to product **2** via the corresponding hydrate, after loss of CH_3OH . This is consistent with the incorporation of ^{18}O from labelled water. That **1** undergoes a photochemical reaction whereby the hydroxyl group at the 4-position is replaced by a proton (deuteron) from water to yield **4** provides strong evidence for a photoprotonation reaction. However, the mechanistic details for the formation of **4** is not trivial and we can only speculate at this time. For example, formation of **4** could arise via fragmentation of the arenium ion, perhaps initially via loss of hydroxyl radical followed by capture of an electron (possibly from the solvated electrons that are known to be generated in this system, *vide supra*), or some other equivalent mechanism. Another possibility involves capture of an electron by the arenium ion first, followed by loss of hydroxyl radical. This pathway generates an aromatic ring in the cleavage step which is more appealing. Attempts to directly

observe either the hydroxyl radical (or hydrogen peroxide) were unsuccessful, presumably due to its rapid reaction with substrates in the reaction mixture. We believe that a possible driving force for the loss of the 4-OH group is due to decreased steric hindrance (with the neighbouring methoxys) that accompanies the replacement of the hydroxy group with a proton.

The major pathway that has been confirmed for reaction for **1** is a formal *demethoxylation* reaction resulting from $\text{C}_{\text{aryl}}\text{-O}$ cleavage leading to the formation of **2** and CH_3OH . The arenium ion intermediate has a minor resonance contributor with the positive charge distributed onto the methoxy oxygen. We also propose the occurrence of a minor pathway involving nucleophilic attack on the methoxy carbon resulting in $\text{C}_{\text{methyl}}\text{-O}$ cleavage which is formally a *demethylation* reaction (Scheme 2). When chloride ion is present, attack at the methoxy carbon yields CH_3Cl and the keto form of **2**. Presumably, attack of chloride ion on the ring carbon also occurs, but is reversible leading back to starting material. Since the quantum yield for the production of methanol is at least three orders of magnitude higher than that for CH_3Cl , demethoxylation by water is clearly the major pathway.

Photochemical reactions involving aromatic ring protonations followed by demethoxylations have been reported previously by Wan and co-workers [24]. In general, the photochemically induced acid-base chemistry of the aromatic ring has been associated with the singlet excited state of aromatic ring systems containing electron donating groups. For example, 1,2-dimethoxybenzene, 1,3-dimethoxybenzene and 1,4-dimethoxybenzene have been shown to undergo photoprotonation in acidic aqueous media ($\text{pH} < 2$) as demonstrated by isotope labelling studies, which revealed exchange of ring protons in the reaction product. In addition, 1,2-dimethoxybenzene also exhibited *ipso* substitution of the methoxy group by water as shown by ^{18}O labelling experiments [24].

The photoprotonation mechanism agrees well with the photolysis of the related compounds and the observed pH effect. Indeed, for compound **5**, products arising via initial protonation at carbons 3 and 4 were observed. Since the photoprotonation must be a result of increased basicity of the aromatic ring, an electron donating substituent would be required to introduce negative charge into the ring. The carboxylate substituent along with the hydroxy and methoxy groups present in **1** are donating enough to increase the excited state basicity of the ring to allow the protonation to occur. The influence of the hydroxy and methoxy groups was evidenced by the lack of similar reactivity exhibited by compounds **4** and **9**. The three donating groups on **1** would also be important in stabilizing the ground state arenium ion intermediate. Since **4** and **9** were

lacking all three donating groups, the intermediate would not have been effectively stabilized.

The photochemistry of lignins and a variety of model compounds containing the syringyl moiety have been previously studied [11c,27,28]. In some of this work, a demethoxylation pathway was attributed to the formation of a phenoxyl radical, which initiated the loss of the methoxy group. In the case of syringic acid, Moore [12e] has suggested that photodecarboxylation and oxidation leading to a quinone derivative or the polymerization phenoxyl radicals may play a role in the production of CH_3Cl . We have ruled out the possibility of a radical cation intermediate as inconsistent with our experimental results. In particular, oxidation leading to radical cation intermediates would be expected to readily form phenoxyl radicals in water due to the extremely low pK_a of the phenol radical cation in aqueous media [29]. Based on this, it would be virtually impossible for the radical cation of **1** to demethoxylate since it would rapidly deprotonate to form the phenoxyl radical. In addition, it is well known that water is typically not a strong enough nucleophile to allow photosubstitution to occur on anisole derivatives, thus discounting the radical cation substitution. Instead, we have proposed a mechanism for the aqueous photochemistry of **1** that accounts for the production of **2** and **4** as well as the release of both CH_3OH and CH_3Cl (in chloride enriched water) via a common photoprotonated intermediate.

Acknowledgments

This research was supported by the Natural Sciences and Engineering Research Council (NSERC) of Canada through the Discovery Grant and USRA programs, Vancouver Island University and the University of Victoria. EK and CG acknowledge the Canada Foundation for Innovation for infrastructure funding to establish the Applied Environmental Research Laboratories at VIU. We also thank Owen Stechishin for carrying out preliminary MIMS experiments.

Appendix A. Supplementary data

Supplementary data associated with this article can be found, in the online version, at doi:10.1016/j.jphotochem.2009.07.023.

References

- [1] (a) R.A. Larson, E.J. Weber, Reaction Mechanisms in Environmental Organic Chemistry, CRC, Boca Raton, 1994;
(b) J.A. Leenheer, J.P. Croue, Environ. Sci. Technol. 37 (2003) 18A.
- [2] (a) W. Flaig, H. Beutelspacher, E. Rietz, in: J.E. Gieseking (Ed.), Soil Components, Springer, Berlin/Heidelberg/New York, 1975;
(b) J.M. Bollag, J. Dec, P.M. Huang, Advances in Agronomy, vol. 63, Academic Press Inc., San Diego, 1998;
(c) G. Abbt-Braun, U. Lankes, F.H. Frimmel, Structural Characterization of Aquatic Humic Substances, Birkhauser Verlag Ag, Basel, 2004.
- [3] (a) J.F. Power, D.K. Sharma, C.H. Langford, R. Bonneau, J. Jousset-Dubien, Photochem. Photobiol. 44 (1986) 11;
(b) W.J. Cooper, R.G. Zika, R.G. Petasne, A.M. Fischer, ACS Symp. Ser. 219 (1989) 333;
(c) J. Hoigne, B.C. Faust, W.R. Haag, F.E. Scully, R.G. Zepp, ACS Symp. Ser. 219 (1989) 363;
(d) J.P. Aguer, C. Richard, F. Andreux, Analusis 27 (1999) 387;
- (e) C.L. Osburn, D.P. Morris, K.A. Thorn, R.E. Moeller, Biogeochemistry 54 (2001) 251.
- [4] J.P. Aguer, C. Richard, J. Photochem. Photobiol. A 93 (1996) 193.
- [5] W.R. Haag, J. Hoigne, Environ. Sci. Technol. 20 (1986) 341.
- [6] R.G. Zepp, A.M. Braun, J. Hoigne, J.A. Leenheer, Environ. Sci. Technol. 21 (1987) 485.
- [7] R.M. Baxter, J.H. Carey, Nature 306 (1983) 575.
- [8] (a) W. Graneli, M. Lindell, B.M. De Faria, F.D. Esteves, Biogeochemistry 43 (1998) 175;
(b) A.E.D. Machado, R. Ruggiero, M.G. Neumann, J. Photochem. Photobiol. A 81 (1994) 107.
- [9] W.J. Cooper, R.G. Zika, Science 220 (1983) 711.
- [10] S. Punshon, R.M. Moore, Mar. Chem. 108 (2008) 215.
- [11] (a) J. Dec, K. Haider, J.M. Bollag, Soil Sci. 166 (2001) 660;
(b) P. Ander, M.E.R. Eriksson, K.E. Eriksson, Physiol. Plant 65 (1985) 317;
(c) O. Lanzalunga, M. Bietti, J. Photochem. Photobiol. B 56 (2000) 85.
- [12] (a) F. Keppler, R. Eiden, V. Niedan, J. Pracht, H.F. Scholer, Nature 403 (2000) 298;
(b) D.B. Harper, Nat. Prod. Rep. 17 (2000) 337;
(c) R.M. Moore, The Handbook of Environmental Chemistry, vol. 3, Springer, New York, 2003 (part P);
(d) R.M. Moore, O.C. Zafiriou, J. Geophys. Res.: Atmos (1994) 16415;
(e) R.M. Moore, Environ. Sci. Technol. 42 (2008) 1933.
- [13] D.J. Jacob, B.D. Field, Q.B. Li, D.R. Blake, J. de Gouw, C. Warneke, A. Hansel, A. Wisthaler, H.B. Singh, A. Guenther, Global budget of methanol: constraints from atmospheric observations, J. Geophys. Res.: Atmos. 110 (2005) 17.
- [14] B.G. Heikes, W.N. Chang, M.E.Q. Pilson, E. Swift, H.B. Singh, A. Guenther, D.J. Jacob, B.D. Field, R. Fall, D. Riemer, L. Brand, Glob. Biogeochem. Cycle 16 (2002) 13.
- [15] J. Williams, R. Holzinger, V. Gros, X. Xu, E. Atlas, D.W.R. Wallace, Geophys. Res. Lett. 31 (2004) 5.
- [16] D.B. Millet, D.J. Jacob, T.G. Custer, J.A. de Gouw, A.H. Goldstein, T. Karl, H.B. Singh, B.C. Sive, R.W. Talbot, C. Warneke, J. Williams, Atmos. Chem. Phys. 8 (2008) 6887.
- [17] (a) R.M. Moore, W. Groszko, S.J. Niven, J. Geophys. Res.: Oceans 101 (1996) 28529;
(b) M.A.K. Khalil, R.M. Moore, D.B. Harper, J.M. Lobert, D.J. Erickson, V. Koropalov, W.T. Sturges, W.C. Keene, J. Geophys. Res.: Atmos 104 (1999) 8333.
- [18] (a) J.H. Seinfeld, S.N. Pandis, Atmospheric Chemistry and Physics, John Wiley and Sons, New York, 1998;
(b) M.J. Molina, F.S. Rowland, Nature 249 (1974) 810;
(c) S. Solomon, Nature 347 (1990) 347.
- [19] J.M. Lobert, W.C. Keene, J.A. Logan, R. Yevich, J. Geophys. Res.: Atmos. 104 (1999) 8373.
- [20] R. Watling, D.B. Harper, Mycol. Res. 102 (1998) 769.
- [21] R.C. Rhew, B.R. Miller, R.F. Weiss, Nature 403 (2000) 292.
- [22] Y. Yokouchi, M. Ikeda, Y. Inuzuka, T. Yukawa, Nature 416 (2002) 163.
- [23] (a) R. Benner, S. Opsahl, Org. Geochem. 32 (2001) 597;
(b) S. Opsahl, R. Benner, Limnol. Oceanogr. 43 (1998) 1297.
- [24] R. Pollard, S. Wu, G.Z. Zhang, P. Wan, J. Org. Chem. 58 (1993) 2605.
- [25] (a) L.E. Slivon, M.R. Bauer, J.S. Ho, W.L. Budde, Anal. Chem. 63 (1991) 1335;
(b) J.H.L. Nelson, E.T. Krogh, C.G. Gill, D.A. Friesen, J. Environ. Sci. Health A 39 (2004) 2307;
(c) J.M. Etkorn, N.G. Davey, A.J. Thompson, A.S. Creba, C.W. LeBlanc, C.D. Simpson, E.T. Krogh, C.G. Gill, J. Chromatogr. Sci. 47 (2009) 57.
- [26] (a) T. Stalin, N. Rajendiran, Spectrosc. Acta Pt. A: Mol. Biomol. Spectr. 61 (2005) 3087;
(b) Advanced Chemistry Development, Inc., ACD/pKa DB, Toronto, Canada, www.acdlabs.com/products/phys_chem_lab/pka/.
- [27] (a) M.G. Neumann, R. Degroote, A.E.H. Machado, Polym. Photochem. 7 (1986) 401;
(b) M.G. Neumann, R. Degroote, A.E.H. Machado, Polym. Photochem. 7 (1986) 461;
(c) A.M. McNally, E.C. Moody, K. McNeill, Photochem. Photobiol. Sci. 4 (2005) 268.
- [28] (a) K. Forest, P. Wan, C.M. Preston, Photochem. Photobiol. Sci. 3 (2004) 463;
(b) C. Crestini, M. Dauria, J. Photochem. Photobiol. A 101 (1996) 69;
(c) C.M. Felicio, A.E.D. Machado, A. Castellan, A. Nourmamode, D.D. Perez, R. Ruggiero, J. Photochem. Photobiol. A 156 (2003) 253.
- [29] M.R. Ganapathi, S. Naumov, R. Hermann, O. Brede, Chem. Phys. Lett. 337 (2001) 335.